

QUEELS software package for calculation of surface effects in electron spectra

S. Tougaard^{1*} and F. Yubero²

¹ Physics Institute, University of Southern Denmark, DK-5230 Odense M, Denmark

² Instituto de Ciencia de Materiales de Sevilla, Isla de la Cartuja, E-41092 Sevilla, Spain

Received 29 July 2003; Revised 6 November 2003; Accepted 7 November 2003

Surface analysis based on the interpretation of electron spectroscopy such as x-ray photoelectron spectroscopy, Auger electron spectroscopy, or reflection electron energy loss spectroscopy are influenced by the inelastic scattering processes that take place when an electron moves in the region near a solid surface. The actual energy losses depend on the particular experimental situation. Thus, an electron is attracted by its image charge when it is moving in the vacuum. It will therefore lose energy even after it has left the surface and, similarly, an electron that moves in the vacuum towards the solid surface gains energy. Likewise, the scattering properties for an electron moving close to the surface are different from those of an electron moving in the bulk of the solid. In photoemission and Auger experiments the effect of the static hole will also affect the scattering probabilities of the electron in the first few ångströms as it moves away from the point of excitation. These effects will also cause the 'effective' inelastic mean free path to depend on the position of the electron with respect to the surface and with respect to the point of excitation. In the past years, we have developed models to describe these effects within a dielectric response theory for different cases of electrons moving near surfaces in general geometries with or without a static core hole. The formulas are quite involved with many infinite integrals and this is a major barrier for people to apply them in practice. With the purpose of making the calculations easier to perform, we have developed software (QUEELS: QUantitative analysis of Electron Energy Losses at Surfaces) that will do this in a user-friendly way. It is hoped that with this tool at hand, we will be able to more effectively and quickly get a more complete understanding of the importance of these different effects for quantitative analysis of surface electron energy spectra. Copyright © 2004 John Wiley & Sons, Ltd.

KEYWORDS: surface effects; XPS; REELS; software; IMFP; dielectric function

INTRODUCTION

The energy distribution of electrons emitted from solid surfaces depends on the inelastic scattering properties of the solid. The surface itself gives rise to special energy loss processes. The energy spectra of emitted photon-excited electrons and Auger excited electrons are also affected by the core holes that are left behind at the point of excitation.

Schematic representations of different situations in which an electron interacts with their surroundings near to a surface are shown in Fig. 1. Thus, Fig. 1(a) shows a static situation where the charge of an electron at rest is screened by the surrounding electrons of the solid and an electric field is set up. Figure 1(b) shows the situation where the electron is moving in the solid. This gives rise to a time-varying electric field and the electrons of the solid may respond to this by electronic excitations. The excitation energy is taken from the moving electron which, in turn, loses energy. Figure 1(c) shows the situation where the electron gets close to the surface. Here the spatial extension of the electric field is

modified by the presence of the surface. After the electron has left the surface it will still induce charge redistributions in the solid and the electron will interact with this field and may thus still lose energy while it moves outside the solid in the vacuum after it has left the surface as in Fig. 1(d). Figure 1(e) shows the situation where there are one or two static core-holes left behind at the point of excitation corresponding to a photon-excited or Auger excited electron, respectively. The Auger electron or photoelectron will interact with the electric field from these static positive charges in the first few ångströms as it moves away which, in turn, will change the probability distribution for energy loss.

Several research groups have been involved in the development of models to describe these processes. Thus, back in 1954, Lindhard¹ described the energy losses of electrons moving in an infinite medium. A few years later, Ritchie² used a hydrodynamical model to describe losses of electrons travelling through a thin film corresponding to the situation in transmission electron energy loss spectroscopy (TEELS). In the 1970s and early 1980s Flores, Echenique *et al.*^{3,4} were very active in the development of models for electron energy losses in different geometries. On the other hand Arista and co-workers^{5,6} used the specular reflection

*Correspondence to: S. Tougaard, Physics Institute, University of Southern Denmark, DK-5230 Odense M, Denmark.
E-mail: svt@fysik.sdu.dk

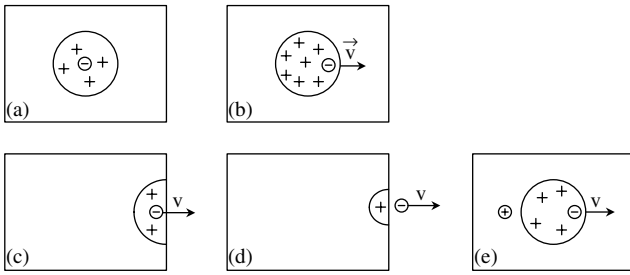


Figure 1. Different experimental situations that give rise to different boundary conditions for the calculations of energy loss processes.

model to interpret electron losses. Several other authors have also contributed with models.^{7–15}

Following the works of Lindhard and Ritchie we have, in the 1990s, developed models based on a dielectric response description of the interaction between the moving electron and the electrons and possible core hole in solids.^{16–18} Thus, we have presented models to reproduce theoretically spectra obtained within reflection electron energy loss spectroscopy (REELS) and XPS using a dielectric description of the interaction between the moving electron and the electrons in the surface region where it travels. Some of the equations are complicated and involve several infinite integrations and this has been a main hindrance for widespread practical use of the results. We have therefore decided to make an effort to implement the resulting algorithms into a user-friendly software package that will facilitate the practical use of these models. We hope that, with this software at hand, it will be possible to more effectively and quickly reach a better level of understanding of the importance of these processes for quantitative analysis of surface electron spectra. The present paper serves as a reference for these future investigations. After an initial thorough testing it is the plan to make the QUEELS software generally available.

BRIEF DESCRIPTION OF THE THEORETICAL BACKGROUND

Figure 2 shows the experiments of main practical interest for TEELS, REELS, XPS and AES analysis. It is exactly these situations that are modelled by the present software. We consider an electron moving in a trajectory corresponding to one of these situations with energy E_0 nearby the surface region of a solid characterized by a dielectric function ϵ . The probability that this electron shall lose energy $\hbar\omega$ ($\hbar\omega \ll E_0$) per unit energy loss and per unit path length is the so-called effective inelastic cross-section $K_{\text{eff}}^{\text{bc}}(E_0, \hbar\omega; \epsilon, x_i^{\text{bc}})$. The trajectory of the moving electron and the surroundings of the electron–surface system define the boundary conditions (bc) of the problem. Thus, x_i^{bc} refers to the particular parameters that describe the interaction between the moving electron and the surface. For example, for an electron moving in a V-type backscattering geometry (as happens in REELS experiments for most electrons having undergone a single inelastic scattering event), it refers to the incoming and outgoing angles and the depth at which the backscattering takes place, or in the case of a photoelectron emission, to

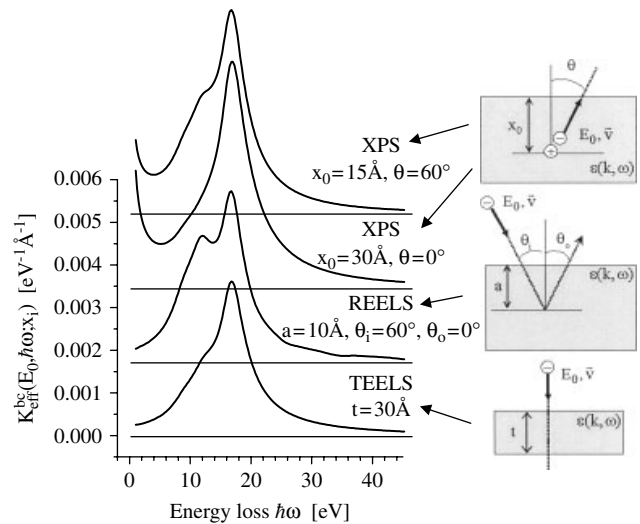


Figure 2. Calculated cross-section for electrons of 1000 eV travelling the same distance 30 Å inside a Si sample but in different geometries.

the depth at which the emission takes place and the angle of emission. $K_{\text{eff}}^{\text{bc}}(E_0, \hbar\omega; \epsilon, x_i^{\text{bc}})$ can be described in terms of the induced potential $\Phi_{\text{ind}}^{\text{bc}}(k, \omega; \epsilon, x_i^{\text{bc}})$ set up by the moving electron in a particular trajectory within the surface region of a solid, with initial energy E_0 and velocity \vec{v} . Thus, it is found that¹⁶

$$K_{\text{eff}}^{\text{bc}}(E_0, \hbar\omega; \epsilon, x_i^{\text{bc}}) = \frac{2}{(2\pi)^4 x \hbar^2 \omega} \int_{-\infty}^{\infty} dt \int d^3 r \rho_e(\vec{r}, t) \text{Re} \times \left\{ i \int d^3 k \vec{k} \cdot \vec{v} \Phi_{\text{ind}}^{\text{bc}}(\mathbf{k}, \omega; \epsilon, x_i^{\text{bc}}) \times e^{i(\vec{k}\vec{r} - \omega t)} \right\} \quad (1)$$

where $\rho_e(\vec{r}, t)$ is the charge density that describes the moving electron, x is the path length travelled inside the medium, and t , \mathbf{r} and \mathbf{k} are time, space and momentum variables of integration. The induced potential is found by solving the Poisson equation in Fourier space with the appropriate boundary conditions corresponding to the particular experimental situation. Note that very different situations must be considered: the existence of one or two surfaces crossed by the electron, the occurrence of a backscattering event at a given depth, and the presence of none, one or two static holes that affect the energy losses of the moving electron.

The case of describing energy losses for an electron moving in an infinite medium is easily calculated within this model and results in the well-known expression

$$K_{\text{eff, bulk}}(E_0, \hbar\omega; \epsilon) = \frac{1}{\pi a_0 E_0} \int \frac{dk}{k} \text{Im}\{1/\epsilon(\mathbf{k}, \omega)\}$$

The other cases get increasingly more complex. In all cases, it is however possible to isolate different contributions in the final cross-section and identify terms corresponding to losses due to the interaction of the moving electron with the bulk material $K_{\text{eff, bulk}}$ and correcting terms related to the interaction of the moving electron with the presence of the

surface $K_{\text{eff,surface}}^{\text{bc}}$ and possible static holes $K_{\text{eff,hole}}^{\text{bc}}$. The actual expressions of these latter two depend on the particular boundary conditions considered in each case.

The QUEELS software allows one to evaluate each of these terms for the case of electrons travelling through a thin film, in a back-reflected geometry and photoemission and Auger emission from a surface. Thus, the effective cross-section $K_{\text{eff}}^{\text{bc}}$ can be expressed as $K_{\text{eff}}^{\text{bc}} = K_{\text{eff,bulk}} + K_{\text{eff,surface}}^{\text{bc}}$ where $K_{\text{eff,surface}}^{\text{bc}}$ indicates the correction to $K_{\text{eff,bulk}}$ induced by the presence of the boundary conditions (the surface and, for XPS and AES, the static core hole).

It is also possible within the applied model to formally identify, for each of these contributions to the cross-section, the excitations that originate from excitations that take place as the electron moves in the vacuum and inside the medium:

$$K_{\text{eff,surface}}^{\text{bc}} = K_{\text{eff,medium}}^{\text{bc}} + K_{\text{eff,vacuum}}^{\text{bc}}$$

Each of these contributions is calculated by the software and this thus gives a quite detailed picture of the different contributions to energy loss.

In the case of REELS or XPS/XAES experiments, one collects electrons that have experienced not only a single trajectory, but a distribution of trajectories. Thus in the case of REELS the backscattering event can take place at different depths in the sample, and in the case of XPS/XAES emission it can take place also at any depth. This can be taken into account for a homogeneous sample, by a weighted average of the previously described effective cross-section as $K_{\text{sc}}^{\text{bc}} = [\int_0^\infty dx Q^{\text{bc}}(x) K_{\text{eff}}^{\text{bc}}] / [\int_0^\infty dx Q^{\text{bc}}(x)]$ where x is the total pathlength travelled by the electron inside the medium and $Q^{\text{bc}}(x)$ is the pathlength distribution function for the electrons considered. In the present software we have used $Q^{\text{bc}}(x) = xe^{-x/\lambda_{\text{eff}}}$, where λ_{eff} is the so-called 'effective' inelastic mean free path. It can be either a fixed value given by the available electron inelastic mean free paths from the literature or a self-consistent value estimated as the inverse of the area of the effective cross-section calculated by the software.

Thus, $K_{\text{sc}}^{\text{REELS}}$ or $K_{\text{sc}}^{\text{XPS/XAES}}$ calculated in this way can be compared directly to the cross-section obtained from multiple scattering background subtraction in experimental REELS and XPS/XAES spectra.

EXAMPLES OF APPLICATIONS

Because of the limited space available here we can only briefly mention a few possible applications. Figure 2 shows the calculated cross-section for electrons of 1000 eV energy travelling 30 Å in Si in different geometries as described in the insets: through a hypothetical thin film 30 Å thick, back-reflected with angle of incidence of 60° and normal angle of emission (with the back-reflection at 10 Å depth), photoemitted at a depth of 30 Å in normal emission, and photoemitted at a depth of 15 Å with angle of emission of 60°. Note that in all cases the electron travels the same distance inside the Si sample. However, the relative intensity of surface vs bulk excitation is quite different in each case. Thus, among the cases depicted in the figure, surface excitations are most enhanced with respect to bulk excitations in the case of electrons travelling in the V-type

trajectory. Besides, note that in XPS at normal emission from 30 Å depth, no significant surface excitations are visible.

Not only can the total cross-sections be calculated but also the contribution due to surface–bulk excitations, excitations induced by the hole, losses taking place in vacuum and inside the medium where the electron travels, depending on the particular case considered. As an example, Fig. 3 shows the decomposition of a particular cross-section for emission as in XPS (Si, $E_0 = 1000$ eV, normal emission, $x_0 = 10$ Å). The contribution to the losses induced by the hole has been isolated. Note that most of the bulk plasmon losses are due to the excitations induced by interaction of the hole with the medium and moving electron. In fact more than half of the bulk plasmon intensity is induced by the presence of the static hole during electron transport.

Besides fundamental studies of energy loss processes in TEELS, REELS, XPS, and AES and calculations of effective inelastic mean free paths, QUEELS can also be applied to determine dielectric properties of bulk materials as well as of thin films. The essence of this method is to vary the parameters describing a parameterized dielectric function until good agreement is found between experimentally determined and theoretically calculated cross-sections. So for each material there will be a unique set of parameters accounting for the dielectric properties. This procedure has been applied to consistently determine the dielectric function of many materials (ZrO₂, Zr, ZrN, TiO₂, SnO₂, Be₃N₂) in the form of thin films.^{19–25} From these dielectric functions, it is also a simple matter to calculate the inelastic mean free path. Finally, it should also be noted that besides these tests, the accuracy of the applied theory behind QUEELS has been tested quantitatively in experimental REELS²⁶ and XPS¹⁸ under wide variations of both the experimental geometry and the electron energy.

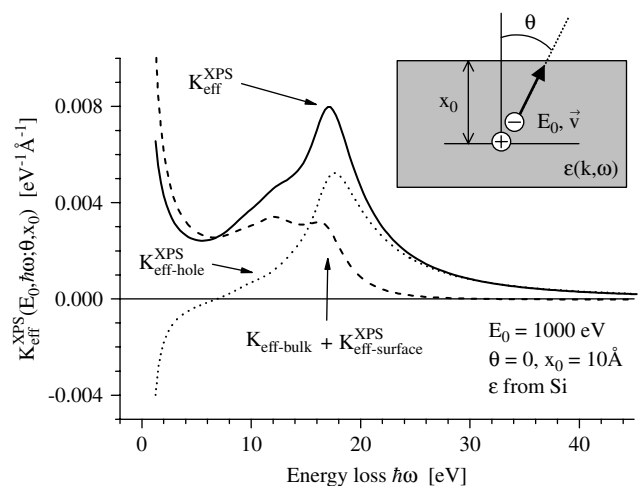


Figure 3. Cross-section for emission in XPS (Si, $E_0 = 1000$ eV, normal emission, $x_0 = 10$ Å). The contribution to the losses induced by the hole has been isolated from that of the electrons.

SUMMARY

The 'Quantitative analysis of electron energy losses at surfaces' (QUEELS) software package is presented. It allows calculations of cross-sections and effective inelastic mean free paths of electrons travelling in different geometries corresponding to XPS, AES, REELS and TEELS experiments, and determination of dielectric functions according to previously presented and tested theory.

REFERENCES

1. Lindhard J. K. *Dan. Vidensk. Selsk. Mat. Fys. Medd.* 1954; **28**: 8.
2. Ritchie RH. *Phys. Rev.* 1957; **106**: 874.
3. Flores F, Garcia-Moliner F. *J. Phys. C Solid State Phys.* 1979; **12**: 907.
4. Echenique PM, Ritchie RH, Barberan N, Inkson J. *Phys. Rev. B* 1981; **23**: 6486.
5. Gervasoni JL, Arista NR. *Surf. Sci.* 1992; **260**: 329.
6. Denton C, Gervasoni JL, Barrachina RO, Arista NR. *Phys. Rev. A* 1998; **57**: 4498.
7. Chen YF, Chen YT. *Phys. Rev. B* 1996; **53**: 4980.
8. Tung CJ, Chen YF, Kwei CM, Chou TL. *Phys. Rev. B* 1994; **49**: 16684.
9. Wang ZL. *Micron* 1996; **27**: 265.
10. Vicanek M. *Surf. Sci.* 1999; **440**: 1.
11. Nagatomi T, Shimizu R, Ritchie RH. *Surf. Sci.* 1999; **419**: 158.
12. Seymour DL, McConville CF, Pand D, Englesfield JE. *Surf. Sci.* 1989; **214**: 57.
13. Mahan GD. *Phys. Rev. B* 1975; **11**: 4814.
14. Ritchie RH, Howie A. *Philos. Mag.* 1977; **36**: 463.
15. Feibelman PJ. *Surf. Sci.* 1973; **36**: 558.
16. Yubero F, Tougaard S. *Phys. Rev. B* 1992; **46**: 2486.
17. Yubero F, Sanz JM, Ramskov B, Tougaard S. *Phys. Rev. B* 1996; **53**: 9719.
18. Simonsen AC, Yubero F, Tougaard S. *Phys. Rev. B* 1997; **56**: 1612.
19. Yubero F, Tougaard S, Elizalde E, Sanz JM. *Surf. Interface Anal.* 1993; **20**: 719.
20. Yubero F, Sanz JM, Trigo JF, Elizalde E, Tougaard S. *Surf. Interface Anal.* 1994; **22**: 124.
21. Prieto P, Yubero F, Elizalde E, Sanz JM. *J. Vac. Sci. Technol. A* 1996; **14**: 3181.
22. Yubero F, Jimenez V, Gonzalez-Elipe AR. *Surf. Sci.* 1998; **400**: 116.
23. Fuentes GG, Mancheño IG, Balbás F, Quirós C, Trigo JF, Yubero F, Elizalde E, Sanz JM. *Phys. Stat. Sol. (a)* 1999; **175**: 429.
24. Cruz W, Soto G, Yubero F. *Opt. Mater.* 2004; **25**: 39.
25. Fuentes GG, Elizalde E, Yubero F, Sanz JM. *Surf. Interface Anal.* 2002; **33**: 230.
26. Yubero F, Fujita D, Ramskov B, Tougaard S. *Phys. Rev. B* 1996; **53**: 9728.